ORIGINAL PAPER

Nagoya J. Med. Sci. **76**. 35 ~ 49, 2014

PREMATURE CARDIAC SENESCENCE IN DahlS.Z-*Lepr*^{fa}/*Lepr*^{fa} RATS AS A NEW ANIMAL MODEL OF METABOLIC SYNDROME

KEIJI TAKAHASHI[1], MS; MIWA TAKATSU[1], MS; TAKUYA HATTORI[1], MS; TAMAYO MURASE[1], MS; SAE OHURA[1], BSC; YUURI TAKESHITA[1], BSC; SHOGO WATANABE[1], PhD; TOYOAKI MUROHARA[2], MD, PhD; and KOHZO NAGATA[1], MD, PhD

[1]*Department of Pathophysiological Laboratory Sciences, Nagoya University Graduate School of Medicine, Nagoya, Japan*
[2]*Department of Cardiology, Nagoya University Graduate School of Medicine, Nagoya, Japan*

ABSTRACT

Aging is accelerated by metabolic and cardiovascular diseases, and the risk of these diseases increases with age. Obesity is an important risk factor for many age-related diseases and is linked to reduced telomere length in white blood cells. We investigated whether cardiac senescence might be enhanced in DahlS.Z-*Lepr*^{fa}/*Lepr*^{fa} (DS/obese) rats, which we recently established as a new animal model of metabolic syndrome. The heart of DS/obese rats was compared with that of homozygous lean littermates (DahlS.Z-*Lepr*$^{+}$/*Lepr*$^{+}$, or DS/lean, rats). DS/obese rats manifested hypertension as well as left ventricular hypertrophy, fibrosis, and diastolic dysfunction at 18 weeks of age. Myocardial oxidative stress and inflammation were increased in DS/obese rats compared with DS/lean rats. Telomere length in myocardial cells did not differ between the two rat strains, whereas telomerase activity and expression of the telomerase reverse transcriptase gene were increased in DS/obese rats. Expression of the senescence-associated genes for checkpoint kinase 2 (Chk2), p53, and p21 as well as that of genes related to the renin-angiotensin-aldosterone system were also up-regulated in the DS/obese rat heart. Our results indicate that DS/obese rats undergo premature cardiac senescence as well as cardiac remodeling in association with the development of diastolic dysfunction in these animals.

Key Words: metabolic syndrome, cardiac remodeling, oxidative stress, renin-angiotensin-aldosterone system, cardiac senescence.

INTRODUCTION

Metabolic syndrome (MetS), a complex of highly debilitating disorders including hypertension, diabetes mellitus, and dyslipidemia, is associated with the development of visceral obesity. Aging is accelerated by metabolic and cardiovascular diseases, and the risk of these diseases increases with age.[1)] Many conditions that increase in prevalence during aging, such as obesity, insulin resistance, inflammation, and hypertension, also contribute to the increase in prevalence of MetS

Received: August 6, 2013; accepted: October 21, 2013

Corresponding author: Kohzo Nagata, MD, PhD
Department of Pathophysiological Laboratory Sciences, Nagoya University Graduate School of Medicine, 1-1-20 Daikominami, Higashi-ku, Nagoya 461-8673, Japan.
Tel./Fax: +81-52-719-1546. E-mail: nagata@met.nagoya-u.ac.jp

and cardiovascular disease. The multiple-organ involvement and increased all-cause mortality characteristic of MetS are reminiscent of a precocious aging process. The mechanisms that account for this phenomenon are incompletely understood, but longevity genes are implicated. Genes thought to determine lifespan include those for mammalian target of rapamycin (mTOR), AMP-activated protein kinase (AMPK), sirtuins, forkhead box O (FOXO) transcription factors, and mediators of insulin and insulin-like growth factor–1 (IGF-1) signaling.

Telomere shortening has been considered a driving force by which genetic and environmental factors jointly affect biological aging and, possibly, the risk for development of age-associated diseases. Telomeres (the extreme ends of chromosomes) shorten progressively during each cell cycle and serve as an indicator of biological age. Reduced telomere length is associated with insulin resistance and obesity, type 1 and type 2 diabetes, hypertension, activation of the renin-angiotensin-aldosterone system (RAAS), and renal failure.[2] Cardiac homeostasis is thought to be dependent on a balance between myocyte loss and proliferation, and aging has been suggested to impair this equilibrium.[3] Consistent with this notion, the number of myocytes with short telomeres is increased in the aging rat heart.[4] However, the relation between MetS and cardiac aging has remained unclear.

We recently established a new animal model of MetS, the DahlS.Z-*Lepr*^{fa}/*Lepr*^{fa} (DS/obese) rat, by crossing Dahl salt-sensitive (DS) rats and Zucker rats with a missense mutation in the leptin receptor gene (*Lepr*).[5] DS/obese rats develop a phenotype similar to MetS in humans, including hypertension, when fed a normal diet. In addition, they develop cardiac hypertrophy as well as renal and liver damage, which may be responsible for their premature death.[5] We have also shown that DS/obese rats develop salt-sensitive hypertension, as well as left ventricular (LV) diastolic dysfunction, hypertrophy, and fibrosis, and that these conditions are accompanied by increased cardiac oxidative stress and inflammation as well as activation of the cardiac RAAS.[6] We have now investigated cardiac senescence and telomere biology in DS/obese rats in comparison with their lean littermates.

METHODS

Animals and experimental protocols

Animal experiments were approved by the Animal Experiment Committee of Nagoya University Graduate School of Medicine (Daiko district, approval nos. 020–028, 021–18, and 022–-012). Animals were handled in accordance with the Regulations for Animal Experiments at Nagoya University as well as with the Guide for the Care and Use of Laboratory Animals [U.S. National Institutes of Health (NIH) publication no. 85–23, revised 1996].

Ten-week-old male inbred DS/obese rats were obtained from Japan SLC Inc. (Hamamatsu, Japan). The animals were fed normal laboratory chow containing 0.36% NaCl, and both the diet and tap water were provided ad libitum throughout the experimental period. At 18 weeks of age, rats were anesthetized by intraperitoneal injection of ketamine (50 mg/kg) and xylazine (10 mg/kg) and were subjected to echocardiographic analysis. The heart was subsequently removed and weighed, and LV tissue was separated for analysis. Age-matched male homozygous lean littermates of DS/obese rats (DahlS.Z-*Lepr*$^{+}$/*Lepr*$^{+}$, or DS/lean, rats) served as control animals.

Blood pressure measurement and echocardiography

Systolic blood pressure (SBP) and heart rate were measured weekly in conscious animals by tail-cuff plethysmography (BP-98A; Softron, Tokyo, Japan). SBP was measured five times at each time point for each rat and the average value was calculated. At 18 weeks of age, rats were

subjected to transthoracic echocardiography, as described previously.[7] M-mode echocardiography was performed with a 12.5-MHz transducer (Xario SSA-660A; Toshiba Medical Systems, Tochigi, Japan). LV end-diastolic (LVDd) and end-systolic (LVDs) dimensions as well as the thickness of the interventricular septum (IVST) and LV posterior wall (LVPWT) were measured, and endocardial fractional shortening (eFS), midwall fractional shortening (mFS), end-systolic wall stress (ESS), relative wall thickness (RWT), and LV mass were calculated as follows: eFS (%) = 100 × [(LVDd – LVDs)/LVDd][8]; mFS (%) = 100 × [(LVDd + LVPWTd/2 + IVSTd/2) – (LVDs + 2Hs)]/(LVDd + LVPWTd/2 + IVSTd/2)[8]; Hs = {[(LVDd + IVSTd/2 + LVPWTd/2)^3– LVDd^3 + LVDs^3]$^{1/3}$ – LVDs}/2[8]; ESS (kdyne/cm^2) = 0.034 × SBP × LVDs/[LVPWTs × (1 + LVPWTs/LVDs)][9]; RWT = (IVST + LVPWT)/LVDd; LV mass (mg) = {1.04 × [(IVST + LVDd + LVPWT)^3 – LVDd^3] × 0.8} + 0.14.[10] LV ejection fraction (LVEF) was calculated with the formula of Teichholz. For assessment of Doppler-derived indices of LV function, both LV inflow and outflow velocity patterns were simultaneously recorded by pulsed-wave Doppler echocardiography. For assessment of LV diastolic function, we calculated the peak flow velocities at the mitral level during rapid filling (E) and during atrial contraction (A), the E/A ratio, the deceleration time (DcT), and the isovolumic relaxation time (IRT). Both the isovolumic contraction time (ICT) and ejection time (ET) were also determined, and the Tei index, which reflects both LV diastolic and systolic function, was calculated as follows: Tei index = (ICT + IRT)/ET.[11]

Histology and immunohistochemistry

LV tissue was fixed in ice-cold 4% paraformaldehyde for 48 h, embedded in paraffin, and processed for histology, as described.[7] To evaluate macrophage infiltration into the LV myocardium, we performed immunostaining for the monocyte-macrophage marker CD68 with frozen sections (thickness, 5 μm) that had been fixed with acetone. Endogenous peroxidase activity was blocked by exposure of the sections to methanol containing 0.3% hydrogen peroxide. Sections were incubated at 4°C first overnight with mouse monoclonal antibodies to CD68 (1:100 dilution of clone ED1; Chemicon, Temecula, CA, USA) and then for 30 min with Histofine Simple Stain Rat MAX PO (Nichirei Biosciences, Tokyo, Japan). Immune complexes were visualized with diaminobenzidine and hydrogen peroxide, and the sections were counterstained with hematoxylin. All image analysis was performed with NIH Scion Image software (Scion, Frederick, MD, USA).

Superoxide production

Nicotinamide adenine dinucleotide phosphate (NADPH)-dependent superoxide production by homogenates of freshly frozen LV tissue was measured with an assay based on lucigenin-enhanced chemiluminescence as described previously.[12] The chemiluminescence signal was sampled every minute for 10 min with a microplate reader (Wallac 1420 ARVO MX/Light; Perkin-Elmer, Waltham, MA, USA), and the respective background counts were subtracted from experimental values. Superoxide production in tissue sections was examined by staining with dihydroethidium (Sigma, St. Louis, MO, USA) as described.[13] Dihydroethidium is rapidly oxidized by superoxide to yield fluorescent ethidium, and the sections were examined with a fluorescence microscope equipped with a 585-nm long-pass filter. As a negative control, sections were incubated with superoxide dismutase (300 U/mL) before staining with dihydroethidium; such treatment prevented the generation of fluorescence signals (data not shown). The average of dihydroethidium fluorescence intensity values was calculated with the use of NIH Image software (ImageJ).

Quantitative RT-PCR analysis

Total RNA was extracted from LV tissue and treated with DNase with the use of a spin-

vacuum total RNA isolation kit (Promega, Madison, WI, USA). Portions of the RNA (2 μg) were subjected to reverse transcription (RT) with the use of a PrimerScript RT Reagent Kit (Takara, Shiga, Japan). The resulting cDNA was subjected to real-time polymerase chain reaction (PCR) analysis with the use of a Prism 7000 Sequence Detector (Perkin-Elmer), as previously described,[14] and with primers and TaqMan probes specific for cDNAs encoding atrial natriuretic peptide (ANP),7) brain natriuretic peptide (BNP),[7] β-myosin heavy chain (β-MHC),[7] collagen type I or type III,[15] transforming growth factor (TGF)–β1,[7] connective tissue growth factor (CTGF),[12] angiotensin-converting enzyme (ACE),[7] the type 1_A receptor for angiotensin II (AT_{1A}),[7] the mineralocorticoid receptor (MR),[12] serum/glucocorticoid-regulated kinase 1 (Sgk1),[6] monocyte chemoattractant protein (MCP)–1,[12] osteopontin,[12] cyclooxygenase (COX)–2,[16] or the $p22^{phox}$,[17] $gp91^{phox}$,[17] $p47^{phox}$,[6] $p67^{phox}$,[6] and Rac[16] subunits of NADPH oxidase. Alternatively, quantitative RT-PCR analysis was performed with the use of SBYR Mix Ex Taq II (Takara), a Thermal Cycler Dice Real Time System II (Takara), and the specific primers listed in Table 1. Reagents for detection of human glyceraldehyde-3-phosphate dehydrogenase (GAPDH) mRNA (Applied Biosystems, Foster City, CA, USA) were used to quantify rat GAPDH mRNA as an internal standard. All data were normalized by the amount of GAPDH mRNA and expressed relative to the normalized value for DS/lean rats.

Telomere length

Telomere length was measured with the use of a Telo TAGGG Telomere Length Assay Kit (Roche, Penzberg, Germany). In brief, purified genomic DNA was digested with the use of a DNeasy Blood & Tissue Kit (Qiagen, Tokyo, Japan), and the DNA fragments were separated by gel electrophoresis, transferred to a nylon membrane, and subjected to hybridization with a digoxigenin-labeled probe specific for telomeric repeats. The membrane was then incubated consecutively with alkaline phosphatase–conjugated antibodies to digoxigenin and the chemiluminescence substrate CDP-star. The average terminal restriction fragment length was determined by comparison of signals with molecular size standards.

Telomerase activity

Telomerase activity was measured with the use of a Telo TAGGG Telomerase PCR $ELISA^{PLUS}$ Kit (Roche). Total protein (1 μg) isolated from LV tissue and quantitated by ultraviolet absorption spectrometry was mixed with a biotinylated telomerase substrate, an optimized anchor-primer, nucleotides, Taq DNA polymerase, and an internal standard, and the mixture was incubated first for 20 min at 25°C to allow primer elongation and then for 5 min at 94°C to inactivate telomerase. After 30 cycles of amplification (30 s at 94°C, 30 s at 50°C, and 90 s at 72°C), the PCR products were divided into two portions, denatured, and subjected to hybridization separately with digoxigenin-labeled detection probes specific either for telomeric repeats or for the internal standard. The resulting products were immobilized on a streptavidin-coated microplate and detected with horseradish peroxidase–conjugated antibodies to digoxigenin and a peroxidase substrate. The absorbance of the samples was measured with the use of a microplate reader (Wallac 1420 ARVO MX/Light, Perkin-Elmer).

Immunoblot analysis

Total protein was isolated from LV tissue and quantitated with the use of the Bradford reagent (Bio-Rad, Hercules, CA, USA). Equal amounts of protein were subjected to SDS-polyacrylamide gel electrophoresis, and the separated proteins were transferred to a polyvinylidene difluoride membrane, as described previously.[18] The membrane was incubated first with a 1:1000 dilution of mouse monoclonal antibodies to p53 (Cell Signaling Technology, Danvers, MA, USA) or

Table 1. Sequences of oligonucleotide primers for quantitative RT-PCR analysis of rat mRNAs.

Target	Sequence	GenBank accession no.
TERT		NM_053423
Forward	5′-TCGATGGCAGGTTCTATGTG-3′	
Reverse	5′-ACAGCTTGTTCTCCATGTCTCC-3′	
TRF-1		NM_001006962
Forward	5′-GAGCCCGCAGGAACTAGAAC-3′	
Reverse	5′-GCTCTTGTGCTCTGACTGTAGG-3′	
TRF-2		NM_001013143
Forward	5′-ATAGCGGGGAGCCACAGAAC-3′	
Reverse	5′-GCCTCTCCATTCTCCTTGGTC-3′	
Chk2		NM_053677
Forward	5′-GCTCGTCCAGAGAAGCTGAC-3′	
Reverse	5′-TTGATGATGCACGGATGATT-3′	
p21		NM_031515
Forward	5′-ATGACTGAGTATAAACTTGTGGTAG-3′	
Reverse	5′-GTGATTCTGAATTAGGTGTATCGTC-3′	
p53		NM_030989
Forward	5′-GATGTTCCGAGAGCTGAATGAGG-3′	
Reverse	5′-GAGTGAGCCCTGCTGTCTCC-3′	
IGF-1		NM_001082477
Forward	5′-CAACTCTGCCCAATGGTAACTTG-3′	
Reverse	5′-CCGGAACAGATAGCCATCCTG-3′	
Ku70		NM_139080
Forward	5′-GAGCCCTGACACAAATGGAG-3′	
Reverse	5′-GCTCGTCTTCACCCTGAGATT-3′	
Ku80		NM_177419
Forward	5′-AGCGTGAAACCATAGGAAAG-3′	
Reverse	5′-CAGTTGGTCTTGGCTGAATG-3′	
FOXO1		NM_001191846
Forward	5′-CATCACCAAGGCCATCGAGAG-3′	
Reverse	5′-CACTCTTCACCATCCACTCGTAG-3′	
FOXO3		NM_001106395
Forward	5′-AGACCACCCACCTTTTCTTCC-3′	
Reverse	5′-CTGAGCGAGTCCGAAGTGAG-3′	

Abbreviations: TERT, telomerase reverse transcriptase; TRF-1, telomere repeat–binding factor–1; TRF-2, telomere repeat–binding factor–2; Chk2, checkpoint kinase 2; IGF-1, insulin-like growth factor–1; FOXO, forkhead box O.

a 1:1000 dilution of rabbit polyclonal antibodies to GAPDH (Cell Signaling Technology) and then with a 1:1000 dilution of horseradish peroxidase–conjugated goat antibodies to mouse or rabbit immunoglobulin G (Cell Signaling Technology). Detection and quantification of immune complexes were performed as described.[18)]

Statistical analysis

Data are presented as means ± SEM. Differences between groups of rats at 18 weeks of age were assessed with the Mann-Whitney U test. The time courses of body weight, SBP, or heart rate were compared between groups with two-way repeated-measures ANOVA. A P value of <0.05 was considered statistically significant.

RESULTS

Physiological analysis, LV geometry, and cardiac function

Body weight and SBP were significantly higher, whereas heart rate was significantly lower, in DS/obese rats than in DS/lean rats as shown in female DS/obese rats.[6)] Echocardiography revealed that IVST, LVPWT, LVEF, LV mass, and RWT were significantly increased in DS/obese rats compared with DS/lean rats at 18 weeks of age. Whereas eFS was increased and ESS was decreased in DS/obese rats compared with DS/lean rats, mFS did not differ significantly between the two groups. DcT and IRT, both of which are indices of LV relaxation, were significantly increased in DS/obese rats, whereas E/A, which is also an index of LV relaxation, was decreased in these animals compared with DS/lean rats. The Tei index, an overall index of LV contraction and relaxation, was also significantly increased in DS/obese rats compared with DS/lean rats. These results thus showed that LV diastolic function is impaired in DS/obese rats.[6)]

Cardiomyocyte hypertrophy as well as cardiac fibrosis and gene expression

The cross-sectional area of LV cardiomyocytes was greater in DS/obese rats than in DS/lean rats (Figure 1A, Table 2). Hemodynamic overload also resulted in significant up-regulation of the expression of ANP, BNP, and β-MHC genes in the DS/obese rat heart (Table 3). Azan-Mallory staining revealed that fibrosis in perivascular and interstitial regions of the LV myocardium was increased in DS/obese rats compared with DS/lean rats (Figure 1B, C, Table 2). The abundance of collagen types I and III mRNAs, as well as the amounts of TGF–β1 and CTGF mRNAs, which correlate with cardiac fibrosis and growth,[19)] were also increased in DS/obese rats (Table 3).

Cardiac oxidative stress

Superoxide production in myocardial tissue sections revealed by staining with dihydroethidium as well as the activity of NADPH oxidase in LV homogenates were significantly increased for DS/obese rats compared with DS/lean rats (Figure 1D, Table 2). The expression of genes for the $p22^{phox}$ and $gp91^{phox}$ membrane components and for the $p47^{phox}$, $p67^{phox}$, and Rac1 cytosolic components of NADPH oxidase in the left ventricle was also up-regulated in DS/obese rats (Table 3).

Cardiac inflammation

Immunostaining of the LV myocardium for the monocyte-macrophage marker CD68 revealed that the number of CD68-positive cells was increased in DS/obese rats compared with DS/lean rats (Figure 1E, Table 2). The expression of MCP–1, osteopontin, and COX–2 genes in the left ventricle was also up-regulated in DS/obese rats (Table 3).

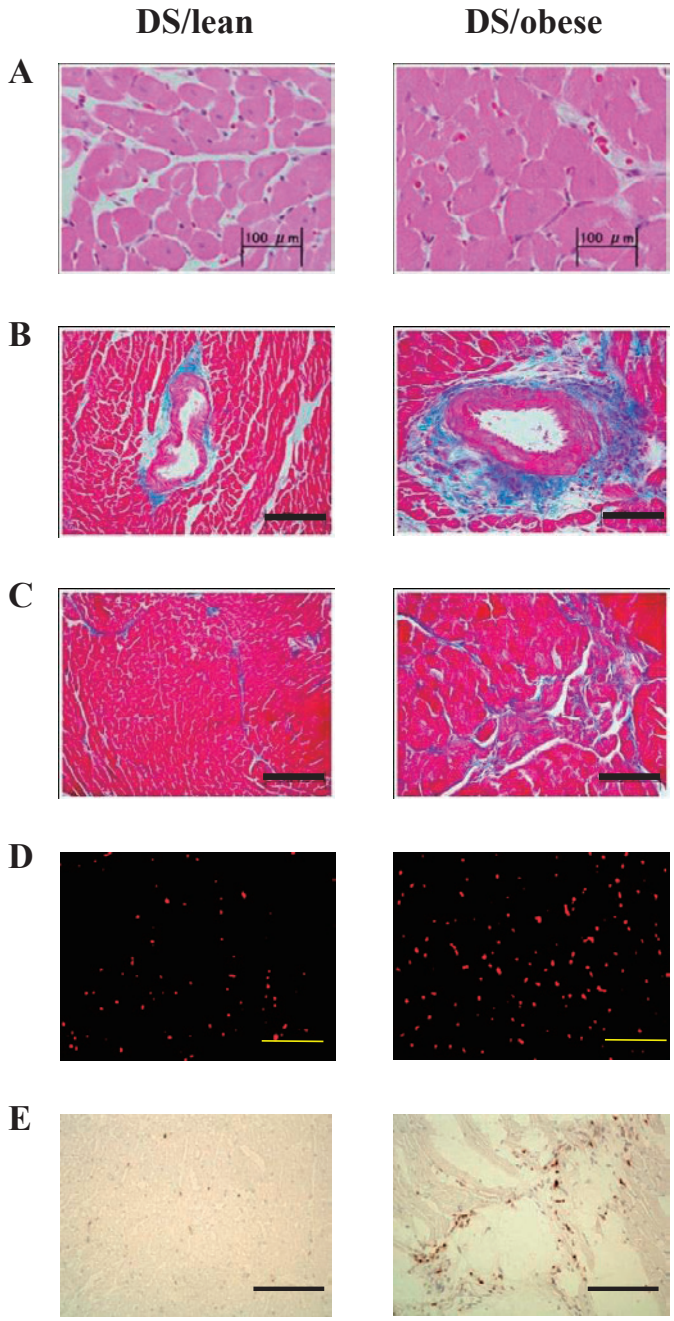

Fig. 1. Cardiomyocyte size, cardiac fibrosis, NADPH oxidase activity and macrophage infiltration in the left ventricle of DS/obese and DS/lean rats at 18 weeks of age. (**A**) Hematoxylin-eosin staining of transverse sections of the LV myocardium. Scale bars, 100 μm. (**B**, **C**) Collagen deposition as revealed by Azan-Mallory staining in perivascular (**B**) and interstitial (**C**) regions of the LV myocardium. Scale bars, 200 μm. (**D**) Superoxide production as revealed by dihydroethidium staining in the LV myocardium. Scale bars, 100 μm. (**E**) Immunohistochemical analysis with antibodies to the monocyte-macrophage marker CD68. Scale bars, 200 μm.

Table 2. Parameters of cardiac hypertrophy, fibrosis, oxidative stress and inflammation in DS/lean and DS/obese rats at 18 weeks of age.

Parameter	DS/lean	DS/obese	*P*
Myocyte cross-sectional area (μm^2)	588±54.3	749±36.2*	0.0184
perivascular fibrosis	0.76±0.07	1.26±0.06*	0.0055
Interstitial fibrosis (%)	3.9±1.1	6.6±0.5*	0.0180
Relative fluorescence intensity (%)	2.4±0.5	7.1±0.7*	0.0021
NADPH oxidase activity (RLU/mg protein)	283±60	1150±121*	0.0023
CD68-positive cells/mm^2	60±3.7	162±22*	0.0041

Data are means ± SEM (n = 4 and 6 for DS/lean and DS/obese rats, respectively). *P < 0.05 versus DS/lean.

Table 3. Cardiac gene expression in DS/lean and DS/obese rats at 18 weeks of age.

Parameter	DS/lean	DS/obese	P
ANP	798±250	2949±823*	<0.0001
BNP	996±144	1594±252*	<0.0001
β-MHC	265±72	411±50*	<0.0001
Collagen type I	363±155	1179±391*	0.0002
Collagen type III	180±45	356±95*	0.0039
TGF-β1	564±156	1017±116*	<0.0001
CTGF	642±72	2372±593*	<0.0001
$p22^{phox}$	7.0±4.5	19.0±5.1*	0.0152
$gp91^{phox}$	25±6.9	92±17.1*	0.0049
$p47^{phox}$	2030±435	4526±1665*	<0.0001
$p67^{phox}$	1719±386	4390±1523*	0.0230
Rac1	1690±385	3580±343*	<0.0001
MCP-1	60±6.7	129±30.3*	0.0036
Osteopontin	11±3.4	32±5.9*	0.0011
COX-2	66±2.5	102±17.4*	0.0457
ACE	118±29.9	396±57.5*	<0.0001
AT_{1A}	58±5.34	164±24.3*	0.0007
MR	1552±269	4063±675*	<0.0001
Sgk1	128±48.5	396±60.6*	<0.0001

Data are means ± SEM (n = 4 and 6 for DS/lean and DS/obese rats, respectively). *P < 0.05 versus DS/lean.

Cardiac RAAS

Cardiac expression of ACE, AT_{1A}, MR, and Sgk1 genes was significantly up-regulated in DS/obese rats compared with DS/lean rats (Table 3).

Telomere biology and markers of cellular aging

Whereas telomere length in the LV myocardium did not differ significantly between DS/obese and DS/lean rats (Figure 2A, B), both telomerase activity (Figure 2C) and the abundance of the mRNA for telomerase reverse transcriptase (TERT) (Figure 2D), the catalytic subunit of telomerase, were increased in DS/obese rats. Expression of the genes for telomere repeat–binding factor–1 (TRF-1) and TRF-2, both of which directly bind to the TTAGGG repeats of telomeres, tended to be increased and decreased, respectively, in DS/obese rats compared with DS/lean rats (Figure 3A, B).

The amounts of mRNAs for checkpoint kinase 2 (Chk2), which mediates cell cycle arrest and apoptosis in response to DNA damage, for the proapoptotic transcription factor p53, and for the p53 target p21 were increased in the LV myocardium of DS/obese rats (Figure 3C–E). The abundance of p53 protein in the left ventricle was also increased in DS/obese rats (Figure 3F). Expression of the gene for IGF-1, which promotes cellular senescence via a reactive oxygen species (ROS)–p53 pathway, tended to be increased in DS/obese rats compared with DS/lean

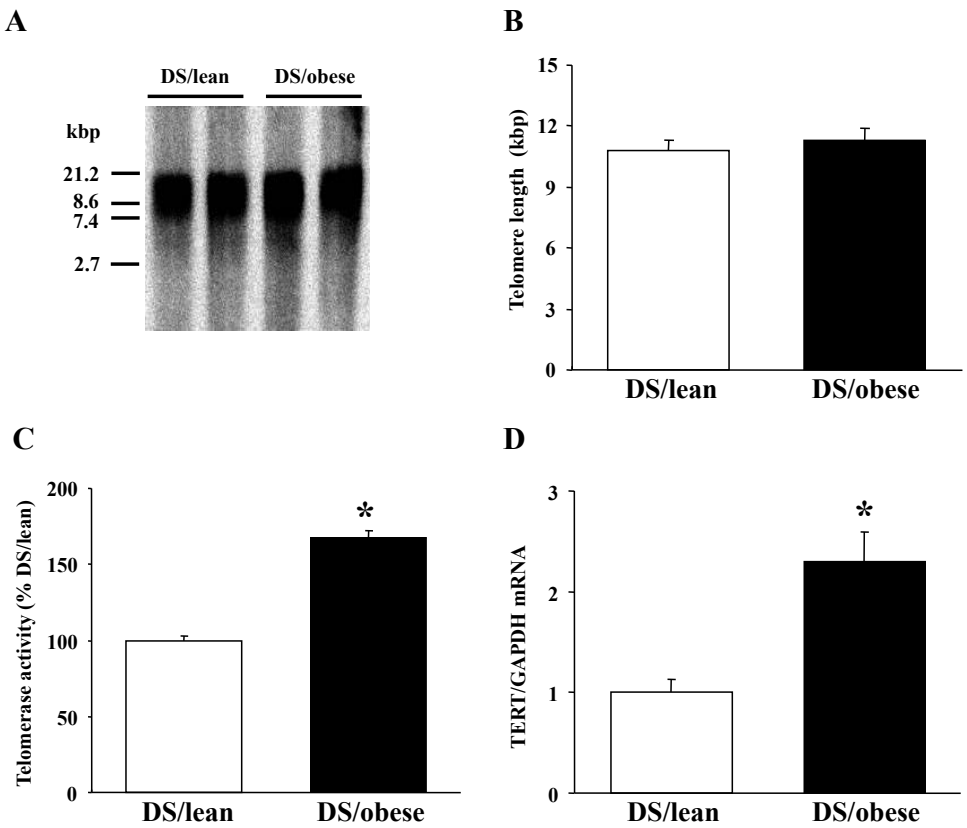

Fig. 2. Telomere length, telomerase activity, and TERT gene expression in the left ventricle of DS/obese and DS/lean rats at 18 weeks of age. (**A**) Representative Southern blot for determination of telomere length. (**B**) Telomere length. (**C**) Telomerase activity determined by a telomere repeat amplification protocol. (**D**) Quantitative RT-PCR analysis of TERT mRNA. All quantitative data are means ± SEM [n = 4 and 4 (**B**), n = 6 and 8 (**C**), and n = 4 and 6 (**D**) for DS/lean and DS/obese rats, respectively]. *$P < 0.05$ versus DS/lean.

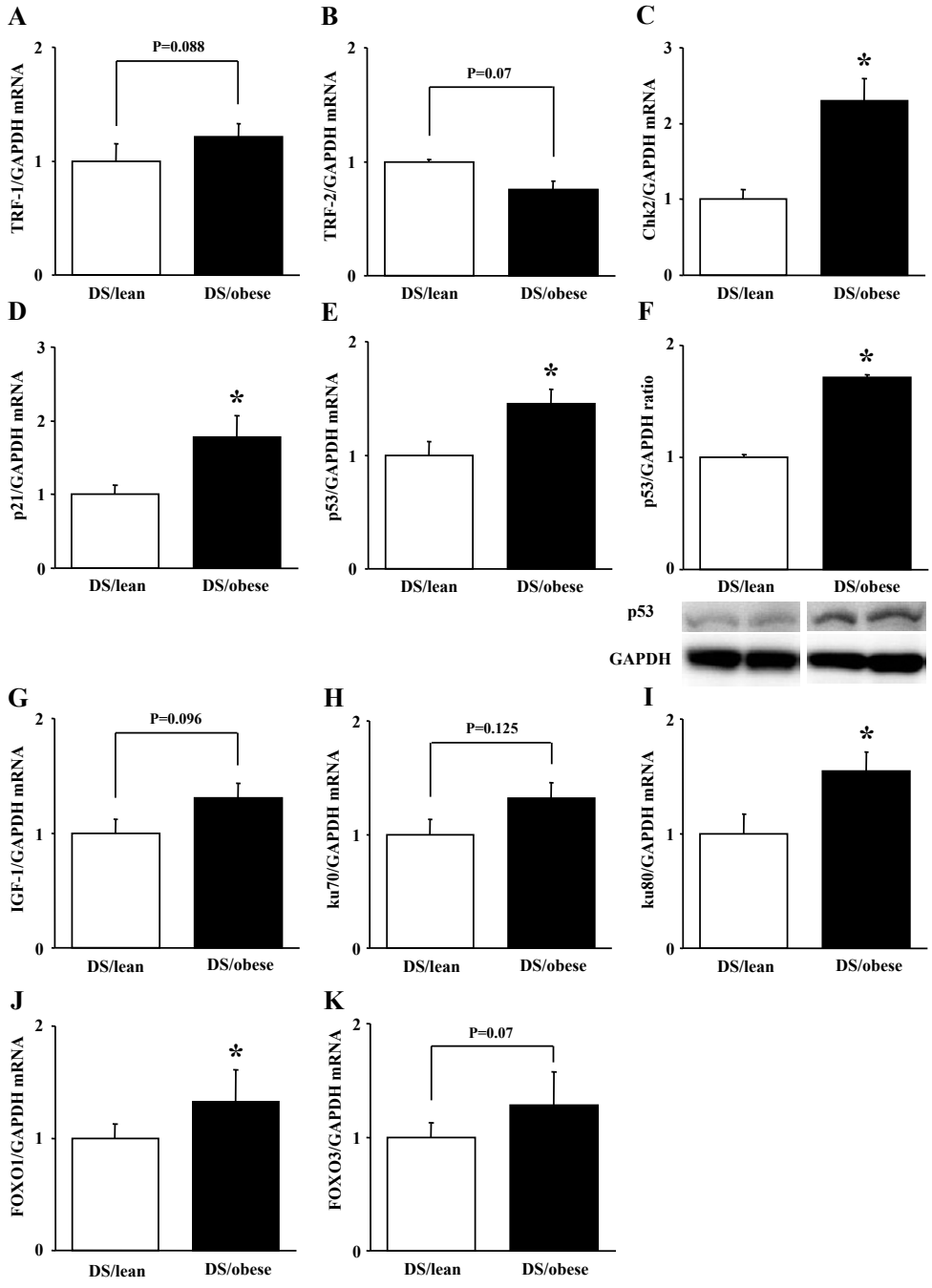

Fig. 3. Expression of aging-related genes in the left ventricle of DS/obese and DS/lean rats at 18 weeks of age. (**A**–**E**, **G**–**K**) Quantitative RT-PCR analysis of TRF-1, TRF-2, Chk2, p21, p53, IGF-1, Ku70, Ku80, FOXO1, and FOXO3 mRNAs, respectively. (**F**) Immunoblot analysis of p53 in the left ventricle. A representative immunoblot and the relative ratio of the amount of p53 to that of GAPDH are shown. All quantitative data are means ± SEM (n = 4 and 6 for DS/lean and DS/obese rats, respectively). *P < 0.05 versus DS/lean.

rats (Figure 3G). The amounts of the mRNAs for the DNA repair protein Ku80 and for the transcription factor FOXO1 were increased in DS/obese rats, whereas that for FOXO3 mRNA tended to be increased in these animals and that for Ku70 mRNA did not differ significantly between the two groups (Figure 3H–K). These results were thus suggestive of the induction of premature cardiac senescence in DS/obese rats.

DISCUSSION

We have here shown that male DS/obese rats at 18 weeks of age manifest LV hypertrophy, fibrosis, and diastolic dysfunction as well as cardiac oxidative stress and inflammation and activation of the cardiac RAAS, as we previously showed for DS/obese females at 15 weeks of age.[6] In addition, male DS/obese rats manifested up-regulation of the expression of senescence-related genes such as those for p53 and p21 as well as an increase in telomerase activity in the LV myocardium, whereas telomere length did not differ from that of control animals. Our results suggest that premature cardiac senescence associated with activation of the p53 pathway may compromise cardiac structure and function in DS/obese rats.

Hypertension has been associated with reduced telomere length in leukocytes in some, but not all, studies.[20, 21] Whereas SBP was higher in DS/obese rats than in DS/lean rats at 11 weeks of age and thereafter, telomere length in myocardial cells was similar in the two groups of animals. These results are consistent with the previous observation that, among individuals with type 1 diabetes, telomere length in white blood cells did not differ significantly between those with or without hypertension after adjustment for age. Telomeres are elongated by the ribonucleoprotein enzyme telomerase, which adds TTAGGG repeats to the 3´ end of DNA strands.[2] In rodents, telomerase protects chromosomes from telomere erosion, maintains cell replication, and prevents cell death. Telomerase consists of two core components, TERT and telomerase RNA component (TERC), the latter of which serves as a template for addition of telomeric repeats to DNA strands. Cardiac telomerase activity declines with age, whereas forced expression of telomerase in cardiomyocytes prevents age-associated telomere shortening and thereby promotes cell proliferation and survival. We found that both telomerase activity and expression of the TERT gene were increased in the left ventricle of DS/obese rats compared with DS/lean rats. Under physiological circumstances, telomerase activity is undetectable or present at only low levels in the adult myocardium. Telomerase is active mostly in cycling myocytes that express stem cell antigens, but it is also present in proliferating myocytes without stem cell markers.[22] The number of proliferative cardiomyocytes is increased in individuals with cardiac hypertrophy[22] or ischemic heart failure,[23] although this myocyte regeneration appears insufficient to prevent cardiac dysfunction. The increased myocardial telomerase activity associated with hypertension and cardiac hypertrophy in DS/obese rats may thus have prevented telomere shortening but not LV diastolic dysfunction in these animals. Given that 18 weeks of age is relatively young, it is possible that older DS/obese rats will manifest telomere shortening. However, 13 of 20 (65%) DS/obese rats in the present study had died by 18 weeks of age from cardiac (4 from sudden death) or noncardiac (7 from renal failure and 2 from cerebrovascular events) causes, in the previous study.[5] Our results thus suggest that telomere-dependent cardiac senescence was compensated for by increased myocardial telomerase activity in DS/obese rats, or that these animals develop telomere-independent cardiac senescence.

Cellular senescence was originally described as resulting from the finite replicative lifespan of human somatic cells in culture. Senescent cells undergo irreversible growth arrest, manifest a flattened and enlarged morphology, and express a distinct set of genes, including those for negative

regulators of the cell cycle such as p53 and p21. Such phenotypic characteristics are not observed in quiescent cells and have been implicated in aging and age-associated diseases. The p53 protein is a key mediator of the cellular response to DNA damage and induces expression of the gene for the cyclin-dependent inhibitor p21.[24] We found that the abundance of p53 mRNA and protein as well as that of p21 mRNA were increased in the heart of DS/obese rats, suggesting that the p53–p21 senescence pathway was induced in the myocardial cells. In addition to the induction of senescence through p21, p53 can also initiate the apoptotic pathway.[25] It was recently shown that cardiac angiogenesis contributes to the adaptive mechanism of cardiac hypertrophy and that p53 accumulation plays a key role in the transition from cardiac hypertrophy to heart failure. In the present study, however, we did not examine cadiomyocyte apoptosis or cardiac angiogenesis because LV systolic dysfunction was not apparent in DS/obese rats. Telomeres are highly sensitive to damage by ROS,[26] with oxidative stress being an important inducer of accelerated telomere attrition.[27] We found that activation of the p53 senescence pathway in the heart of DS/obese rats was accompanied by increased oxidative stress (an increase in NADPH-dependent superoxide production) but not by telomere shortening. Telomerase activity was also increased in the DS/obese rat heart. Oxidative stress was found to induce shortening of telomeres and to accelerate the onset of senescence in cultured vascular smooth muscle cells and endothelial cells.[28] Another study showed that chronic oxidative stress compromised telomere integrity, reduced telomerase activity, and promoted the onset of senescence in human endothelial cells.[29] Our results thus suggest that premature cardiac senescence in DS/obese rats might not be mediated by telomere damage but instead may be telomere independent, with such a telomere-independent pathway having previously been shown to operate in human vascular smooth muscle cells.[30]

In a community-based sample, telomere length in leukocytes was inversely related to systemic RAAS activity, especially in individuals with hypertension.[31] In the present study, expression of ACE, AT_{1A}, MR, and Sgk1 genes was increased in the heart of DS/obese rats, indicative of activation of the cardiac RAAS in these animals. Angiotensin II stimulates the intracellular accumulation of ROS in vascular smooth muscle cells via the AT_1 receptor[23, 24]. Enhanced MR signaling in the myocardium also results in increased oxidative stress and inflammation, leading to the development of cardiac remodeling and dysfunction.[6] Furthermore, angiotensin II rapidly induces oxidative DNA damage in human vascular smooth muscle cells, resulting in up-regulation of p53 and a rapid onset of senescence.[30] Angiotensin II was also found to induce vascular cell senescence and inflammation both in vivo and in vitro via up-regulation of p21 expression,[32] with these effects leading to an increase in ROS production.[33] Our results suggest that activation of the cardiac RAAS induces oxidative stress and inflammation in the heart, leading to the induction of premature cardiac senescence, via the p53–p21 pathway in DS/obese rats.

DS/obese rats showed an increased myocardial abundance of mRNA for the DNA repair protein Ku80, suggesting that DNA was damaged in the heart of these animals. Such damage is likely attributable, at least in part, to angiotensin II- or MR-induced oxidative stress. The telomere-binding protein TRF-2 plays a key role in telomere protection, and the abundance of TRF-2 mRNA tended to be decreased in the heart of DS/obese rats. This latter effect might result in telomere dysfunction in the absence of telomere shortening, leading to the observed up-regulation of Chk2, p53, and p21 gene expression.[2]

IGF-1 plays a key role in the regulation of cell growth and proliferation, with reduced IGF-1 signaling having been found to result in growth retardation in humans.[34] In contrast to its deleterious effects on cell growth and proliferation, reduced IGF-1 signaling has beneficial effects on longevity.[35] In the present study, expression of the IGF-1 gene tended to be increased in the heart of DS/obese rats. IGF-1 increases telomerase activity, thereby delaying cellular aging and death.[36] Cardiac overexpression of IGF-1 in transgenic mice increases heart weight.[37] Cardiac

stem cell division was also found to be enhanced, in association with increased telomerase activity and delayed senescence, in IGF-1 transgenic mice.[36] One study showed that reduction of insulin signaling specifically in adipocytes or neuronal cells extends life span, suggesting that insulin/IGF-1 signaling of specific organs is important and may regulate life span, at least in part, in an endocrine manner.[38] On the other hand, suppression of insulin/IGF-1 signaling in a heart-specific manner prevents the age-dependent decline of cardiac function in Drosophila, indicating that insulin/IGF-1 signaling also regulates aging of individual organs[39]. DS/obese rats exhibited insulin resistance, hyperinsulinemia[6] as well as a trend toward up-regulation of IGF-1 gene expression, suggesting that insulin/IGF-1 signaling may have contributed to the development of cardiac senescence in these rats. The p53 protein negatively regulates IGF-1 signaling and biological activity by several mechanisms.[40] On the other hand, IGF-1 induces p53 expression.[41, 42] In addition, a recent study showed that IGF-1 promotes cellular senescence via the ROS-p53 pathway.[43].

In conclusion, DS/obese rats manifest activation of the p53 pathway in the heart as well as hypertension, LV hypertrophy, cardiac fibrosis, and diastolic dysfunction. RAAS-mediated oxidative DNA damage may contribute to activation of this cardiac senescence pathway in these animals. It is also possible that RAAS activation promoted cardiac inflammation via the p53 pathway, leading to increased myocardial fibrosis. Further investigations are required to clarify the molecular mechanisms that underlie MetS and its associated cardiac senescence and injury.

ACKNOWLEDGEMENTS

We thank Tomomi Inoue and Haruka Tsukamoto for technical assistance and Hiromi Ito for her critical review of the manuscript.

Source of Funding: This work was supported by unrestricted research grants from Nippon Boehringer Ingelheim Co. Ltd. (Tokyo, Japan) and Kyowa Hakko Kirin Co. Ltd. (Tokyo, Japan), as well as by Management Expenses Grants from the Japanese government to Nagoya University.

Conflict of Interest: None

REFERENCES

1) Veronica G, Esther RR. Aging, metabolic syndrome and the heart. *Aging Dis.* 2012; 3: 269–279.
2) Wong LS, Oeseburg H, de Boer RA, van Gilst WH, van Veldhuisen DJ, van der Harst P. Telomere biology in cardiovascular disease: the TERC$^{-/-}$ mouse as a model for heart failure and ageing. *Cardiovasc Res.* 2009; 81: 244–252.
3) Beltrami AP, Urbanek K, Kajstura J, Yan SM, Finato N, Bussani R, Nadal-Ginard B, Silvestri F, Leri A, Beltrami CA, Anversa P. Evidence that human cardiac myocytes divide after myocardial infarction. *N Engl J Med.* 2001; 344: 1750–1757.
4) Kajstura J, Pertoldi B, Leri A, Beltrami CA, Deptala A, Darzynkiewicz Z, Anversa P. Telomere shortening is an in vivo marker of myocyte replication and aging. *Am J Pathol.* 2000; 156: 813–819.
5) Hattori T, Murase T, Ohtake M, Inoue T, Tsukamoto H, Takatsu M, Kato Y, Hashimoto K, Murohara T, Nagata K. Characterization of a new animal model of metabolic syndrome: the DahlS.Z-*Lepr^{fa}*/*Lepr^{fa}* rat. *Nutr Diab.* 2011; 1: e1.
6) Murase T, Hattori T, Ohtake M, Abe M, Amakusa Y, Takatsu M, Murohara T, Nagata K. Cardiac remodeling and diastolic dysfunction in DahlS.Z-*Lepr^{fa}*/*Lepr^{fa}* rats: a new animal model of metabolic syndrome. *Hypertens Res.* 2012; 35: 186–193.

7) Nagata K, Somura F, Obata K, Odashima M, Izawa H, Ichihara S, Nagasaka T, Iwase M, Yamada Y, Nakashima N, Yokota M. AT1 receptor blockade reduces cardiac calcineurin activity in hypertensive rats. *Hypertension.* 2002; 40: 168–174.
8) Shimizu G, Hirota Y, Kita Y, Kawamura K, Saito T, Gaasch WH. Left ventricular midwall mechanics in systemic arterial hypertension. Myocardial function is depressed in pressure-overload hypertrophy. *Circulation.* 1991; 83: 1676–1684.
9) Ono K, Masuyama T, Yamamoto K, Doi R, Sakata Y, Nishikawa N, Mano T, Kuzuya T, Takeda H, Hori M. Echo doppler assessment of left ventricular function in rats with hypertensive hypertrophy. *J Am Soc Echocardiogr.* 2002; 15: 109–117.
10) Reffelmann T, Kloner RA. Transthoracic echocardiography in rats. Evalution of commonly used indices of left ventricular dimensions, contractile performance, and hypertrophy in a genetic model of hypertrophic heart failure (SHHF-Mcc-fa^{cp}-Rats) in comparison with Wistar rats during aging. *Basic Res Cardiol.* 2003; 98: 275–284.
11) Tei C, Ling LH, Hodge DO, Bailey KR, Oh JK, Rodeheffer RJ, Tajik AJ, Seward JB. New index of combined systolic and diastolic myocardial performance: a simple and reproducible measure of cardiac function—a study in normals and dilated cardiomyopathy. *J Cardiol.* 1995; 26: 357–366.
12) Nagata K, Obata K, Xu J, Ichihara S, Noda A, Kimata H, Kato T, Izawa H, Murohara T, Yokota M. Mineralocorticoid receptor antagonism attenuates cardiac hypertrophy and failure in low-aldosterone hypertensive rats. *Hypertension.* 2006; 47: 656–664.
13) Elmarakby AA, Loomis ED, Pollock JS, Pollock DM. NADPH oxidase inhibition attenuates oxidative stress but not hypertension produced by chronic ET-1. *Hypertension.* 2005; 45: 283–287.
14) Somura F, Izawa H, Iwase M, Takeichi Y, Ishiki R, Nishizawa T, Noda A, Nagata K, Yamada Y, Yokota M. Reduced myocardial sarcoplasmic reticulum Ca^{2+}-ATPase mRNA expression and biphasic force-frequency relations in patients with hypertrophic cardiomyopathy. *Circulation.* 2001; 104: 658–663.
15) Sakata Y, Yamamoto K, Mano T, Nishikawa N, Yoshida J, Hori M, Miwa T, Masuyama T. Activation of matrix metalloproteinases precedes left ventricular remodeling in hypertensive heart failure rats: its inhibition as a primary effect of Angiotensin-converting enzyme inhibitor. *Circulation.* 2004; 109: 2143–2149.
16) Murase T, Hattori T, Ohtake M, Nakashima C, Takatsu M, Murohara T, Nagata K. Effects of estrogen on cardiovascular injury in ovariectomized female DahlS.Z-*Lepr^{fa}*/*Lepr^{fa}* rats as a new animal model of metabolic syndrome. *Hypertension.* 2012; 59: 694–704.
17) Yamada T, Nagata K, Cheng XW, Obata K, Saka M, Miyachi M, Naruse K, Nishizawa T, Noda A, Izawa H, Kuzuya M, Okumura K, Murohara T, Yokota M. Long-term administration of nifedipine attenuates cardiac remodeling and diastolic heart failure in hypertensive rats. *Eur J Pharmacol.* 2009; 615: 163–170.
18) Xu J, Nagata K, Obata K, Ichihara S, Izawa H, Noda A, Nagasaka T, Iwase M, Naoe T, Murohara T, Yokota M. Nicorandil promotes myocardial capillary and arteriolar growth in the failing heart of Dahl salt-sensitive hypertensive rats. *Hypertension.* 2005; 46: 719–724.
19) Ahmed MS, Oie E, Vinge LE, Yndestad A, Oystein Andersen G, Andersson Y, Attramadal T, Attramadal H. Connective tissue growth factor—a novel mediator of angiotensin II-stimulated cardiac fibroblast activation in heart failure in rats. *J Mol Cell Cardiol.* 2004; 36: 393–404.
20) Demissie S, Levy D, Benjamin EJ, Cupples LA, Gardner JP, Herbert A, Kimura M, Larson MG, Meigs JB, Keaney JF, Aviv A. Insulin resistance, oxidative stress, hypertension, and leukocyte telomere length in men from the Framingham Heart Study. *Aging Cell.* 2006; 5: 325–330.
21) Jeanclos E, Krolewski A, Skurnick J, Kimura M, Aviv H, Warram JH, Aviv A. Shortened telomere length in white blood cells of patients with IDDM. *Diabetes.* 1998; 47: 482–486.
22) Chimenti C, Kajstura J, Torella D, Urbanek K, Heleniak H, Colussi C, Di Meglio F, Nadal-Ginard B, Frustaci A, Leri A, Maseri A, Anversa P. Senescence and death of primitive cells and myocytes lead to premature cardiac aging and heart failure. *Circ Res.* 2003; 93: 604–613.
23) Urbanek K, Torella D, Sheikh F, De Angelis A, Nurzynska D, Silvestri F, Beltrami CA, Bussani R, Beltrami AP, Quaini F, Bolli R, Leri A, Kajstura J, Anversa P. Myocardial regeneration by activation of multipotent cardiac stem cells in ischemic heart failure. *Proc Natl Acad Sci U S A.* 2005; 102: 8692–8697.
24) Wahl GM, Carr AM. The evolution of diverse biological responses to DNA damage: insights from yeast and p53. *Nat Cell Biol.* 2001; 3: E277–E286.
25) Deng Y, Chan SS, Chang S. Telomere dysfunction and tumour suppression: the senescence connection. *Nat Rev Cancer.* 2008; 8: 450–458.
26) Henle ES, Han Z, Tang N, Rai P, Luo Y, Linn S. Sequence-specific DNA cleavage by Fe^{2+}-mediated fenton reactions has possible biological implications. *J Biol Chem.* 1999; 274: 962–971.
27) Kuwahara F, Kai H, Tokuda K, Takeya M, Takeshita A, Egashira K, Imaizumi T. Hypertensive myocardial

fibrosis and diastolic dysfunction: another model of inflammation? *Hypertension.* 2004; 43: 739–745.
28) Matthews C, Gorenne I, Scott S, Figg N, Kirkpatrick P, Ritchie A, Goddard M, Bennett M. Vascular smooth muscle cells undergo telomere-based senescence in human atherosclerosis: effects of telomerase and oxidative stress. *Circ Res.* 2006; 99: 156–164.
29) Kurz DJ, Decary S, Hong Y, Trivier E, Akhmedov A, Erusalimsky JD. Chronic oxidative stress compromises telomere integrity and accelerates the onset of senescence in human endothelial cells. *J Cell Sci.* 2004; 117: 2417–2426.
30) Herbert KE, Mistry Y, Hastings R, Poolman T, Niklason L, Williams B. Angiotensin II-mediated oxidative DNA damage accelerates cellular senescence in cultured human vascular smooth muscle cells via telomere-dependent and independent pathways. *Circ Res.* 2008; 102: 201–208.
31) Vasan RS, Demissie S, Kimura M, Cupples LA, Rifai N, White C, Wang TJ, Gardner JP, Cao X, Benjamin EJ, Levy D, Aviv A. Association of leukocyte telomere length with circulating biomarkers of the renin-angiotensin-aldosterone system: the Framingham Heart Study. *Circulation.* 2008; 117: 1138–1144.
32) Kunieda T, Minamino T, Nishi J, Tateno K, Oyama T, Katsuno T, Miyauchi H, Orimo M, Okada S, Takamura M, Nagai T, Kaneko S, Komuro I. Angiotensin II induces premature senescence of vascular smooth muscle cells and accelerates the development of atherosclerosis via a p21-dependent pathway. *Circulation.* 2006; 114: 953–960.
33) Macip S, Igarashi M, Fang L, Chen A, Pan ZQ, Lee SW, Aaronson SA. Inhibition of p21-mediated ROS accumulation can rescue p21-induced senescence. *Embo J.* 2002; 21: 2180–2188.
34) David A, Hwa V, Metherell LA, Netchine I, Camacho-Hubner C, Clark AJ, Rosenfeld RG, Savage MO. Evidence for a continuum of genetic, phenotypic, and biochemical abnormalities in children with growth hormone insensitivity. *Endocr Rev.* 2011; 32: 472–497.
35) Bartke A. Growth hormone, insulin and aging: the benefits of endocrine defects. *Exp Gerontol.* 2011; 46: 108–111.
36) Torella D, Rota M, Nurzynska D, Musso E, Monsen A, Shiraishi I, Zias E, Walsh K, Rosenzweig A, Sussman MA, Urbanek K, Nadal-Ginard B, Kajstura J, Anversa P, Leri A. Cardiac stem cell and myocyte aging, heart failure, and insulin-like growth factor-1 overexpression. *Circ Res.* 2004; 94: 514–524.
37) Delaughter MC, Taffet GE, Fiorotto ML, Entman ML, Schwartz RJ. Local insulin-like growth factor I expression induces physiologic, then pathologic, cardiac hypertrophy in transgenic mice. *Faseb J.* 1999; 13: 1923–1929.
38) Kenyon C. The plasticity of aging: insights from long-lived mutants. *Cell.* 2005; 120: 449–460.
39) Wessells RJ, Fitzgerald E, Cypser JR, Tatar M, Bodmer R. Insulin regulation of heart function in aging fruit flies. *Nat Genet.* 2004; 36: 1275–1281.
40) Scrable H, Medrano S, Ungewitter E. Running on empty: how p53 controls INS/IGF signaling and affects life span. *Exp Gerontol.* 2009; 44: 93–100.
41) Chen WH, Pellegata NS, Wang PH. Coordinated effects of insulin-like growth factor I on inhibitory pathways of cell cycle progression in cultured cardiac muscle cells. *Endocrinology.* 1995; 136: 5240–5243.
42) Wang PH, Schaaf GJ, Chen WH, Feng J, Prins BA, Levin ER, Bahl JJ. IGF I induction of p53 requires activation of MAP kinase in cardiac muscle cells. *Biochem Biophys Res Commun.* 1998; 245: 912–917.
43) Handayaningsih AE, Takahashi M, Fukuoka H, Iguchi G, Nishizawa H, Yamamoto M, Suda K, Takahashi Y. IGF-I enhances cellular senescence via the reactive oxygen species-p53 pathway. *Biochem Biophys Res Commun.* 2012; 425: 478–484.